Parton Showers and Resummation Workshop PSR19
Erwin Schroedinger Institute, Vienna, June 2019

F Hautmann

TMDs from Parton Branching

- Introduction
- The Parton Branching (PB) method
- Applications: DIS and DY

I. Introduction

TRANSVERSE MOMENTUM DEPENDENT (TMD)
PARTON DISTRIBUTION FUNCTIONS

- Parton correlation functions at non-lightlike distances:

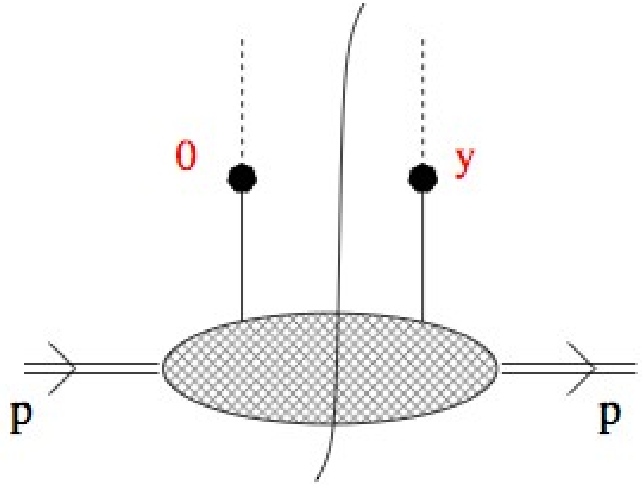

$$p = (p^+ , m^2 / 2 p^+ , 0_\perp)$$

$$\widetilde{f}(y) = \langle \, P \mid \overline{\psi}(y) \; V_y^\dagger(n) \; \gamma^+ \; V_0(n) \; \psi(0) \mid P \, \rangle \quad , \qquad y = (0, y^-, y_\perp)$$

$$V_y(n) = \mathcal{P} \exp \left(i g_s \int_0^\infty d\tau \; n \cdot A(y + \tau \; n) \right)$$

- TMD pdfs:

$$f(x, k_\perp) = \int \frac{dy^-}{2\pi} \frac{d^{d-2} y_\perp}{(2\pi)^{d-2}} e^{-ixp^+ y^- + ik_\perp \cdot y_\perp} \tilde{f}(y)$$

Evolution equations for TMD parton distribution functions

low q_T : $q_T \ll Q$

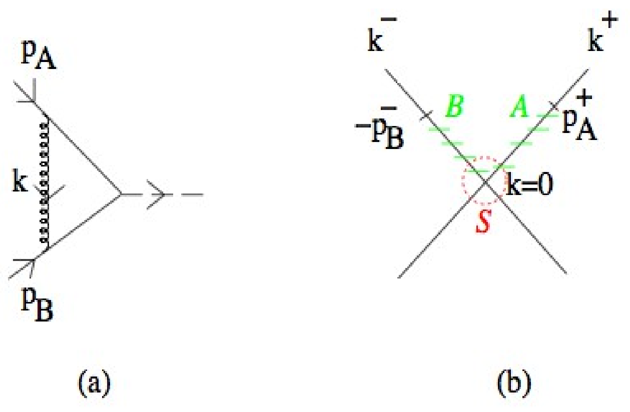

$\alpha_s^n \ln^m Q/q_T$

CSS evolution equation

(or variants – SCET, ...)

high $\sqrt{s}$: $\sqrt{s} \gg M$

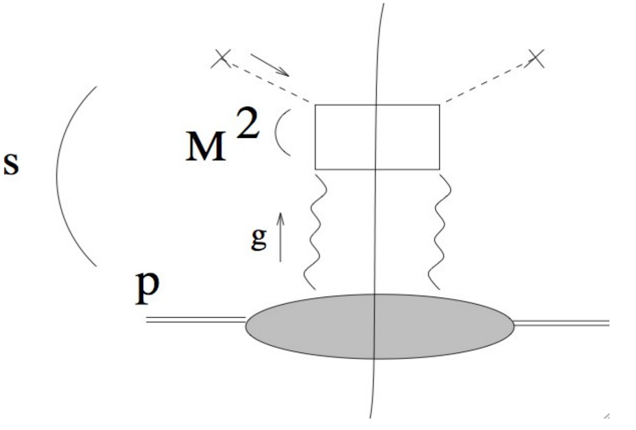

$(\alpha_s \ln \sqrt{s}/M)^n$

CCFM evolution equation

(or BFKL, BK, JIMWLK, …)

R. Angeles-Martinez et al., “Transverse momentum dependent (TMD) parton distribution functions: status and prospects”, Acta Phys. Polon. B46 (2015) 2501

TMD distributions (unpolarized and polarized)

TABLE I

(Colour on-line) Quark TMD pdfs: columns represent quark polarization, rows represent hadron polarization. Distributions encircled by a dashed line are the ones which survive integration over transverse momentum. The shades of the boxes (light gray (blue) *versus* medium gray (pink)) indicate structures that are T-even or T-odd, respectively. T-even and T-odd structures involve, respectively, an even or odd number of spin-flips.

QUARKS	*unpolarized*	*chiral*	*transverse*
U	f_1		$h_1^{\perp}$
L		g_{1L}	$h_{1L}^{\perp}$
T	$f_{1T}^{\perp}$	g_{1T}	h_{1T}, $h_{1T}^{\perp}$

TABLE II

(Colour on-line) Gluon TMD pdfs: columns represent gluon polarization, rows represent hadron polarization. Distributions encircled by a dashed line are the ones which survive integration over transverse momentum. The shades of the boxes (light gray (blue) *versus* medium gray (pink)) indicate structures that are T-even or T-odd, respectively. T-even and T-odd structures involve, respectively, an even or odd number of spin-flips. Linearly polarized gluons represent a double spin-flip structure.

GLUONS	*unpolarized*	*circular*	*linear*
U	f_1^g		$h_1^{\perp g}$
L		g_{1L}^g	$h_{1L}^{\perp g}$
T	$f_{1T}^{\perp g}$	g_{1T}^g	h_{1T}^g, $h_{1T}^{\perp g}$

R. Angeles-Martinez et al., “Transverse momentum dependent (TMD) parton distribution functions: status and prospects”, Acta Phys. Polon. B46 (2015) 2501

Parton Branching (PB) approach

Jung, Lelek, Radescu, Zlebcik & H, "Collinear and TMD quark and gluon densities from parton branching", JHEP 1801 (2018) 070

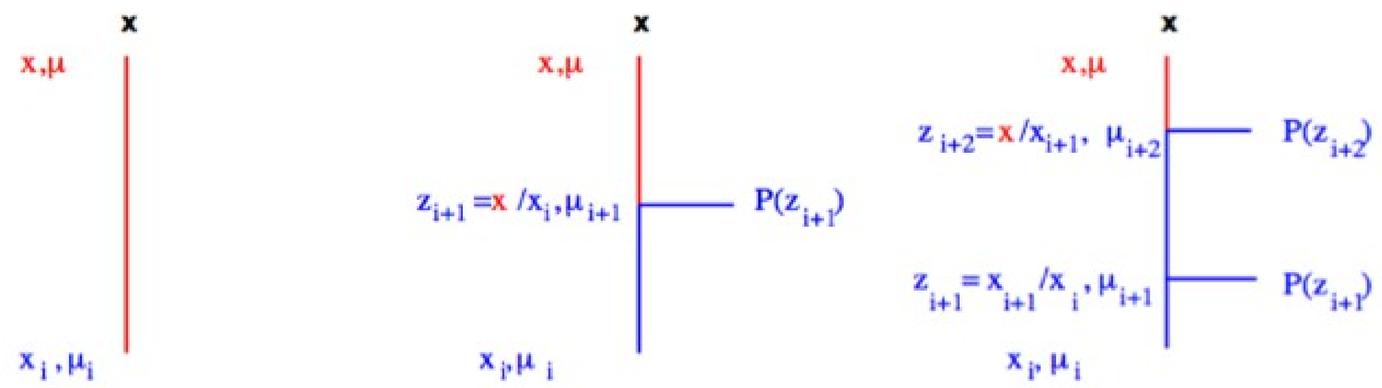

PB evolution equation motivated by

– applicability over large kinematic range from low to high transverse momenta

– applicability to exclusive final states and Monte Carlo event generators

- connection with DGLAP evolution of collinear parton distributions

II. PB method

A new evolution equation for TMDs

$$\mathcal{A}_a(x,\mathbf{k},\mu^2) \;=\; \Delta_a(\mu^2)\,\mathcal{A}_a(x,\mathbf{k},\mu_0^2) + \sum_b \int \frac{d^2\mathbf{q}'}{\pi \mathbf{q}'^2}\,\frac{\Delta_a(\mu^2)}{\Delta_a(\mathbf{q}'^2)}\,\Theta(\mu^2-\mathbf{q}'^2)\,\Theta(\mathbf{q}'^2-\mu_0^2)$$

$$\times \int_x^{z_M} \frac{dz}{z}\,P_{ab}^{(R)}(\alpha_s,z)\,\mathcal{A}_b\left(\frac{x}{z},\mathbf{k}+(1-z)\mathbf{q}',\mathbf{q}'^2\right) \quad ,$$

↖ NB: angular ordering

- solvable by iterative MC technique

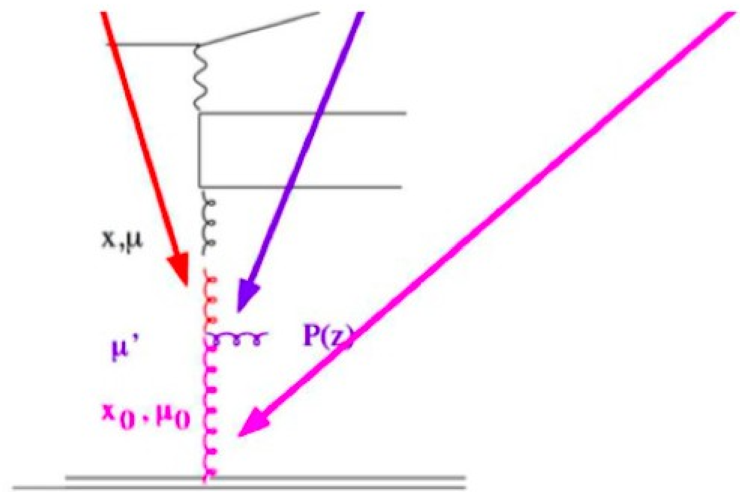

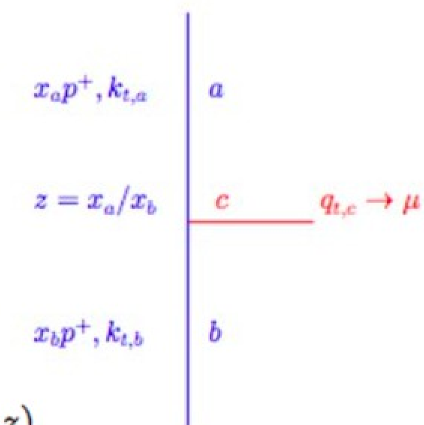

$$\mu = |\mathbf{q}_c|/(1-z)$$

where

$$\Delta_a(z_M,\mu^2,\mu_0^2) = \exp\left(-\sum_b \int_{\mu_0^2}^{\mu^2} \frac{d\mu'^2}{\mu'^2} \int_0^{z_M} dz\, z\, P_{ba}^{(R)}(\alpha_s,z)\right) \quad , \qquad P_{ba}^{(R)}(\alpha_s,z) = \delta_{ba} k_b(\alpha_s)\,\frac{1}{1-z} + R_{ba}(\alpha_s,z)$$

$$k_b(\alpha_s) = \sum_{n=1}^{\infty}\left(\frac{\alpha_s}{2\pi}\right)^n k_b^{(n-1)}, \quad R_{ba}(\alpha_s,z) = \sum_{n=1}^{\infty}\left(\frac{\alpha_s}{2\pi}\right)^n R_{ba}^{(n-1)}(z)$$

Non-resolvable emissions and unitarity method

- Introduce resolution scale z_M, where $1 - z_M \sim \mathcal{O}(\Lambda_{\rm QCD}/\mu)$.

- Classify singular behavior of splitting kernels $P_{ab}(z, \alpha_s)$ in non-resolvable region $1 > z > z_M$:

$$P_{ab}(\alpha_{\rm S}, z) = D_{ab}(\alpha_{\rm S})\delta(1-z) + K_{ab}(\alpha_{\rm S}) \frac{1}{(1-z)_+} + R_{ab}(\alpha_{\rm S}, z)$$

$$\text{where} \quad \int_0^1 \frac{1}{(1-z)_+} \varphi(z) \, dz = \int_0^1 \frac{1}{1-z} \left[\varphi(z) - \varphi(1)\right] dz$$

and $R_{ab}(\alpha_{\rm S}, z)$ contains logarithmic and analytic contributions for $z \to 1$

- Expand plus-distributions in non-resolvable region and use sum rule $\sum_c \int_0^1 z \, P_{ca}(\alpha_{\rm S}, z) \, dz = 0 \ \ (\text{for any } a)$ to eliminate D-terms in favor of K- and R-terms

$\Rightarrow$ real-emission probabilities exponentiate into Sudakov form factors

- angular ordering: q_t = (1 - z) q'

$$k_\perp = -\sum_i q_{\perp,i}$$

PB method: collinear PDFs

QCD evolution and soft-gluon resolution scale

[Jung, Lelek, Radescu, Zlebcik & H, PLB772 (2017) 446 + in progress]

$$\widetilde{f}_a(x,\mu^2) = \Delta_a(\mu^2)\,\widetilde{f}_a(x,\mu_0^2) + \sum_b \int_{\mu_0^2}^{\mu^2} \frac{d\mu'^2}{\mu'^2} \frac{\Delta_a(\mu^2)}{\Delta_a(\mu'^2)} \int_x^{z_M} dz\, P_{ab}^{(R)}(\alpha_s(\mu'^2),z)\,\widetilde{f}_b(x/z,\mu'^2)$$

$$\text{where} \quad \Delta_a(z_M,\mu^2,\mu_0^2) = \exp\left(-\sum_b \int_{\mu_0^2}^{\mu^2} \frac{d\mu'^2}{\mu'^2} \int_0^{z_M} dz\; z\; P_{ba}^{(R)}(\alpha_s(\mu'^2),z)\right)$$

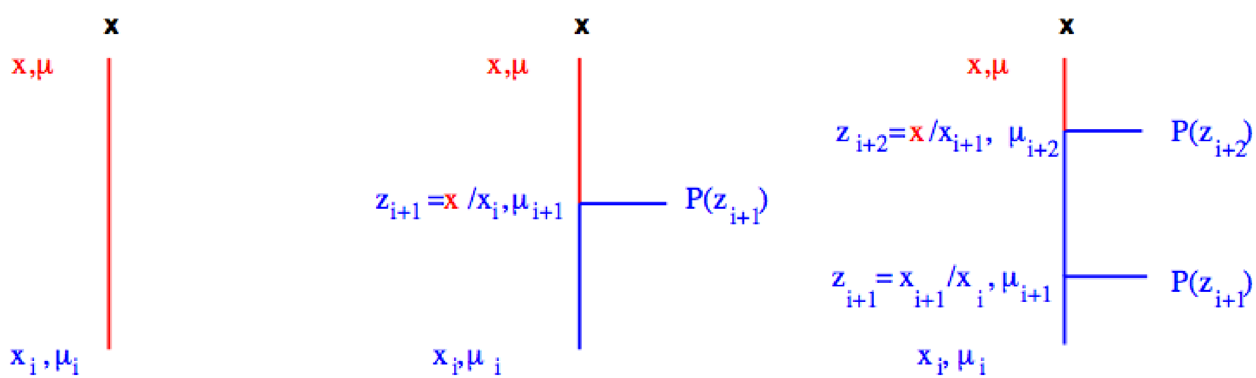

▷ soft-gluon resolution parameter z_M separates resolvable and nonresolvable branchings

▷ no-branching probability Δ; real-emission probability $P^{(R)}$

- Equivalent to DGLAP evolution equation for zM → 1

Validation at LO against semi-analytic result from QCDNUM

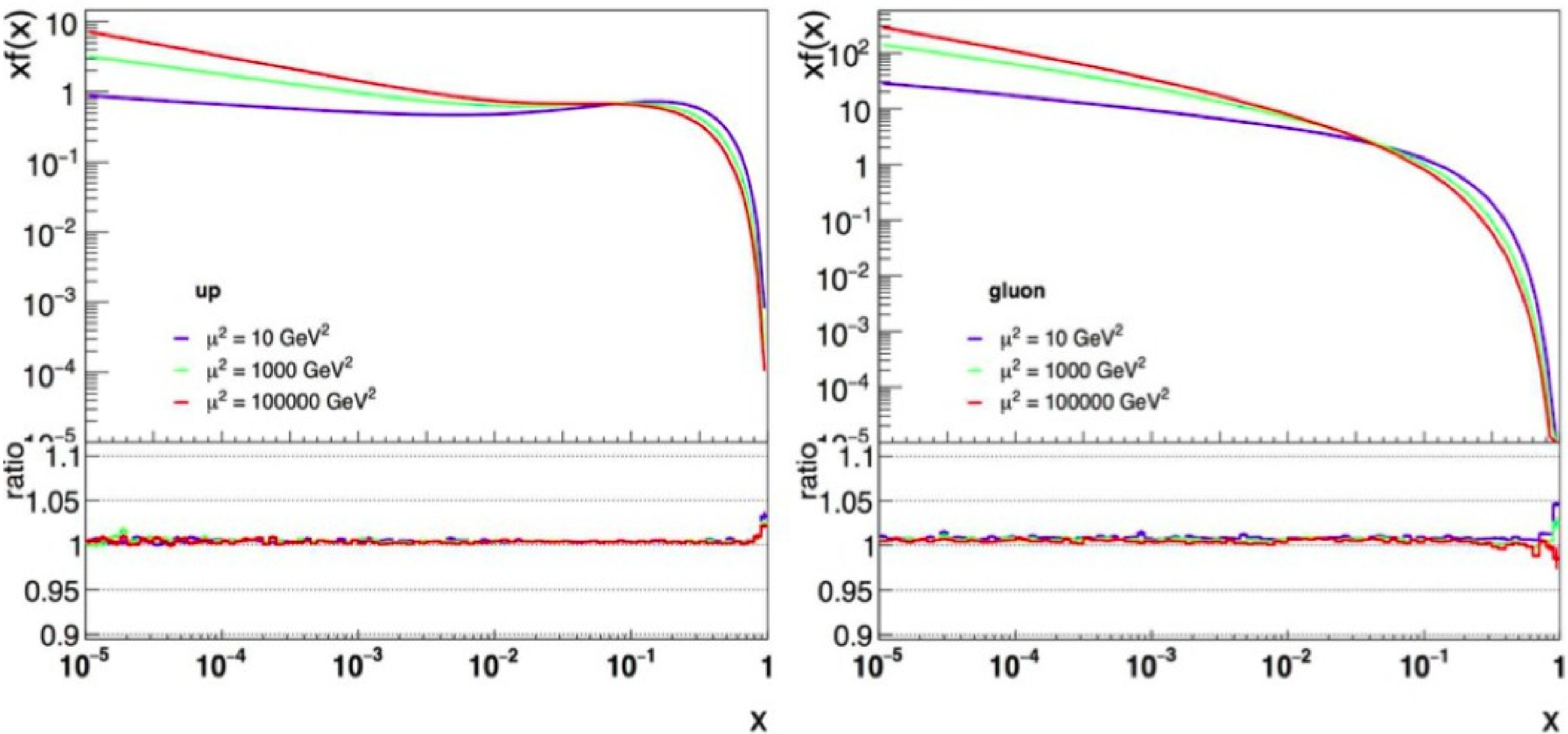

Agreement to better than 1 % over several orders of magnitude in x and mu

See also S. Jadach et al, 2004 – 2010
H. Tanaka et al, 2001 - 2005

Validation at NLO against semi-analytic result from QCDNUM

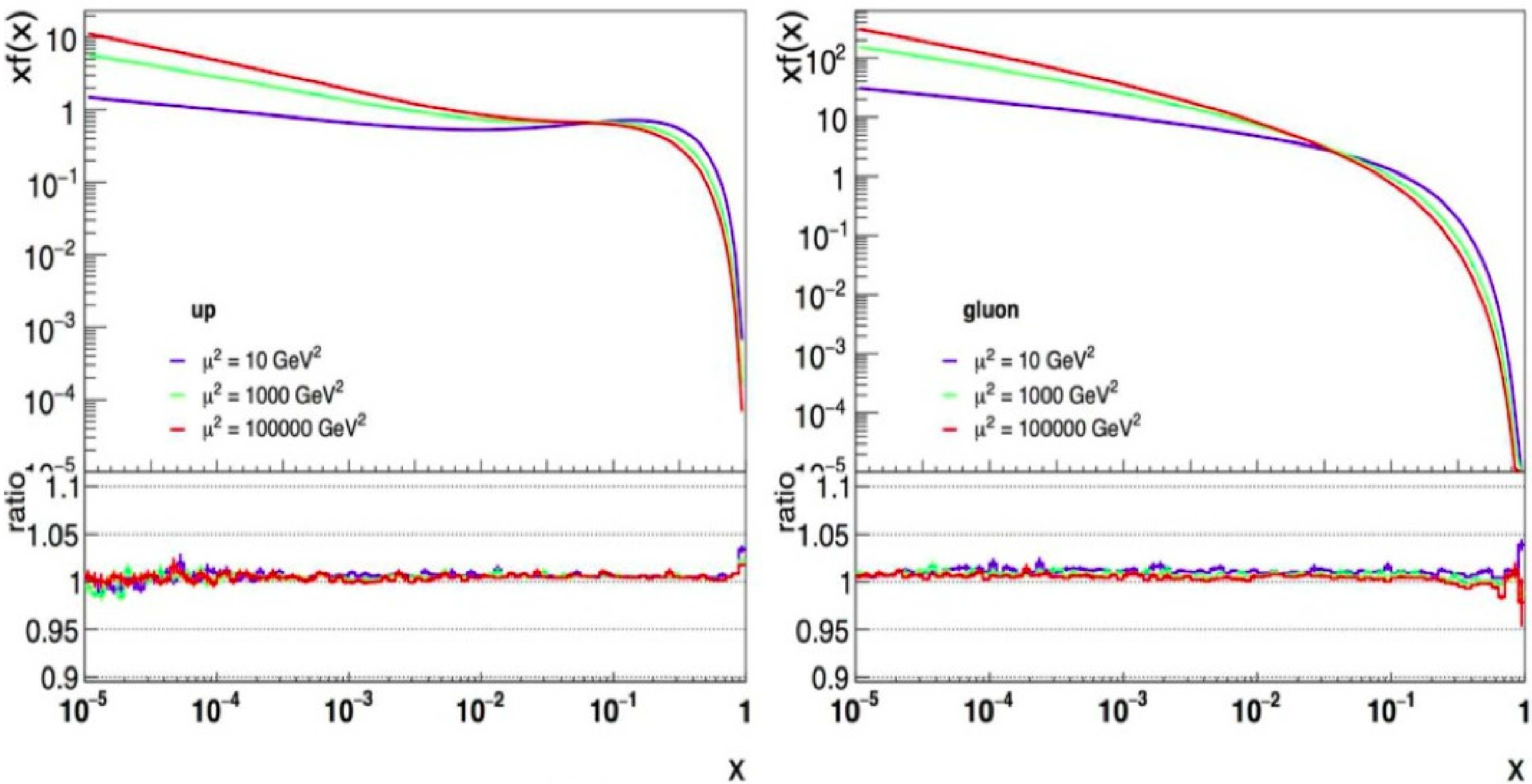

Very good agreement at NLO over all x and mu.
NB: the same approach is designed to work at NNLO.

See also S. Jadach et al, 2004 – 2010
H. Tanaka et al, 2001 - 2005

Stability with respect to resolution scale z_M

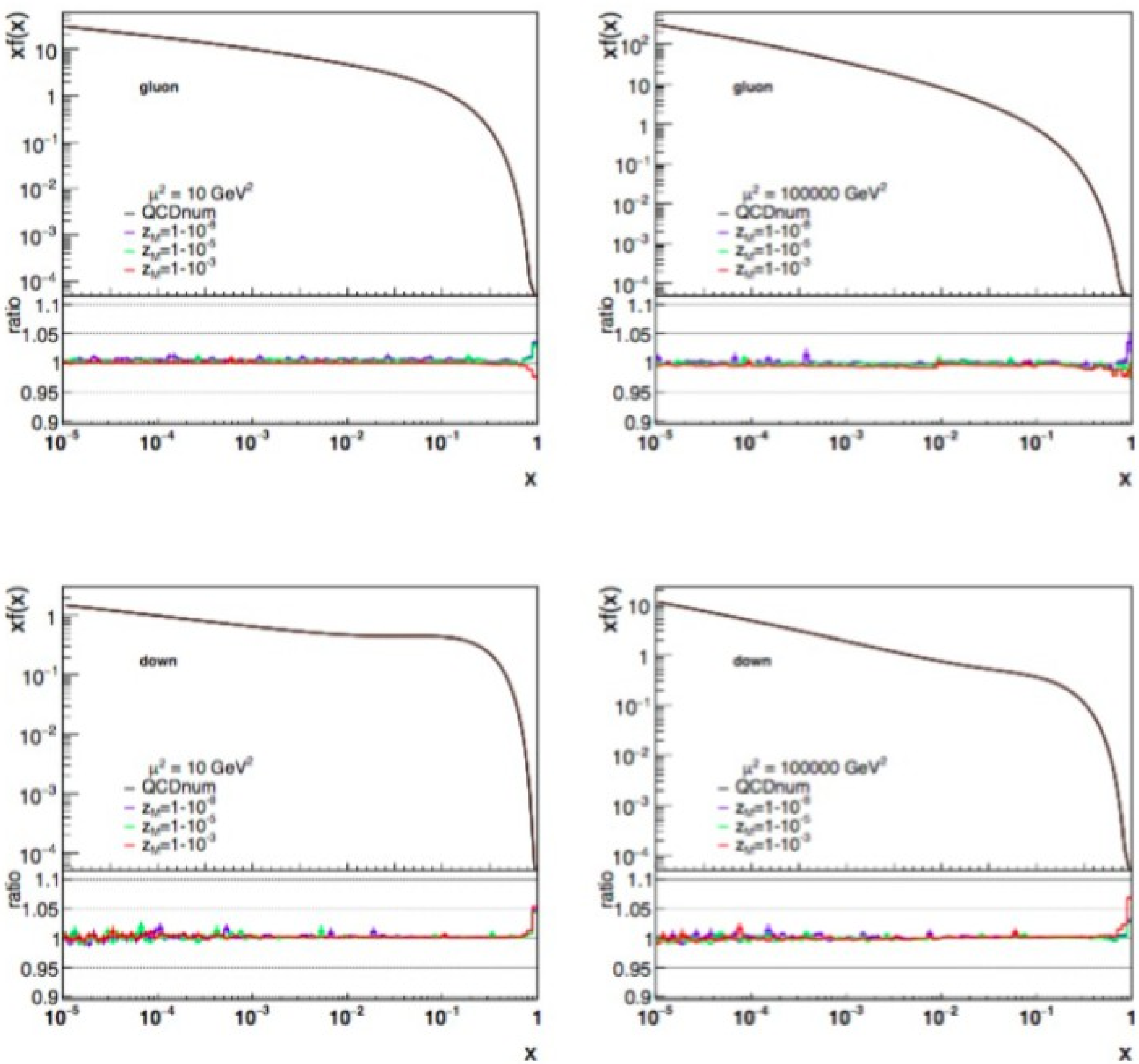

Comparison with CSS (Collins-Soper-Sterman) resummation

◇ The resummed DY differential cross section is given by

$$\frac{d\sigma}{d^2\mathbf{q}dQ^2dy} = \sum_{q,\bar{q}} \frac{\sigma^{(0)}}{s} H(\alpha_S) \int \frac{d^2\mathbf{b}}{(2\pi)^2}\, e^{i\mathbf{q}\cdot\mathbf{b}} \mathcal{A}_q(x_1,\mathbf{b},Q)\mathcal{A}_{\bar{q}}(x_2,\mathbf{b},Q) + \mathcal{O}\left(\frac{|\mathbf{q}|}{Q}\right) \quad \text{where}$$

$$\mathcal{A}_i(x,\mathbf{b},Q) = \exp\left\{\frac{1}{2}\int_{c_0/b^2}^{Q^2} \frac{d\mu'^2}{\mu'^2}\left[A_i(\alpha_S(\mu'^2))\ln\left(\frac{Q^2}{\mu'^2}\right) + B_i(\alpha_S(\mu'^2))\right]\right\} G_i^{(\mathrm{NP})}(x,\mathbf{b})$$
$$\times \sum_j \int_x^1 \frac{dz}{z} C_{ij}\left(z, \alpha_S\left(\frac{c_0}{\mathbf{b}^2}\right)\right) f_j\left(\frac{x}{z}, \frac{c_0}{\mathbf{b}^2}\right)$$

and the coefficients H, A, B, C have power series expansions in α_S.

◇ The parton branching TMD is expressed in terms of real-emission $P^{(R)}$:

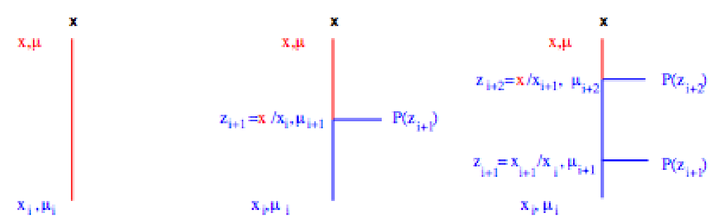

▷ via momentum sum rules, use unitarity to relate $P^{(R)}$ to virtual emission

▷ identify the coefficients in the two formulations, order by order in α_S, at LL, NLL, . . .

Comparison with CSS (Collins-Soper-Sterman) resummation

More precisely:

▷ The parton branching TMD contains Sudakov form factor in terms of

$$P_{ab}^{(R)}(\alpha_s, z) = K_{ab}(\alpha_s)\, \frac{1}{1-z} + R_{ab}(\alpha_s, z) \quad \text{where}$$

$$K_{ab}(\alpha_s) = \delta_{ab} k_a(\alpha_s)\,, \quad k_a(\alpha_s) = \sum_{n=1}^{\infty} \left(\frac{\alpha_s}{2\pi}\right)^n k_a^{(n-1)}\,, \quad R_{ab}(\alpha_s, z) = \sum_{n=1}^{\infty} \left(\frac{\alpha_s}{2\pi}\right)^n R_{ab}^{(n-1)}(z)$$

▷ Via momentum sum rules, use unitarity to re-express this in terms of

$$P^{(V)} = P - P^{(R)}\,, \quad \text{where}$$

$$P_{ab}(\alpha_s, z) = D_{ab}(\alpha_s)\delta(1-z) + K_{ab}(\alpha_s)\, \frac{1}{(1-z)_+} + R_{ab}(\alpha_s, z)$$

is full splitting function (at LO, NLO, etc.)

$$\text{with} \quad D_{ab}(\alpha_s) = \delta_{ab} d_a(\alpha_s)\,, \quad d_a(\alpha_s) = \sum_{n=1}^{\infty} \left(\frac{\alpha_s}{2\pi}\right)^n d_a^{(n-1)}$$

▷ Identify $d_a(\alpha_s)$ and $k_a(\alpha_s)$ with resummation formula coefficients (LL, NLL, . .)

Comparison with CSS (Collins-Soper-Sterman) resummation

- $d_a(\alpha_S)$ and $k_a(\alpha_S)$ perturbative coefficients

$$\text{one-loop}\ :$$

$$d_q^{(0)} = \frac{3}{2}\, C_F \quad , \quad k_q^{(0)} = 2\ C_F$$

$$\text{two-loop}\ :$$

$$d_q^{(1)} = C_F^2 \left(\frac{3}{8} - \frac{\pi^2}{2} + 6\ \zeta(3) \right) + C_F C_A \left(\frac{17}{24} + \frac{11\pi^2}{18} - 3\ \zeta(3) \right) - C_F T_R N_f \left(\frac{1}{6} + \frac{2\pi^2}{9} \right) ,$$

$$k_q^{(1)} = 2\ C_F\ \Gamma\ , \quad \text{where}\ \ \Gamma = C_A \left(\frac{67}{18} - \frac{\pi^2}{6} \right) - T_R N_f \frac{10}{9}$$

- The k and d coefficients of the PB formalism match, order by order, the A and B coefficients of the CSS formalism:

$$\text{LL}\ :\ \ k_q^{(0)} = 2\ C_F = 2\ A_q^{(1)}$$

$$\text{NLL}\ :\ \ k_q^{(1)} = 2\ C_F\ \Gamma = 4\ A_q^{(2)}\ ;\ \ d_q^{(0)} = \frac{3}{2}\, C_F = -B_q^{(1)}$$

$$\text{NNLL}\ :\ \ \text{analysis in progress}$$

Angular ordering in
TMD evolution vs. coherent-branching shower

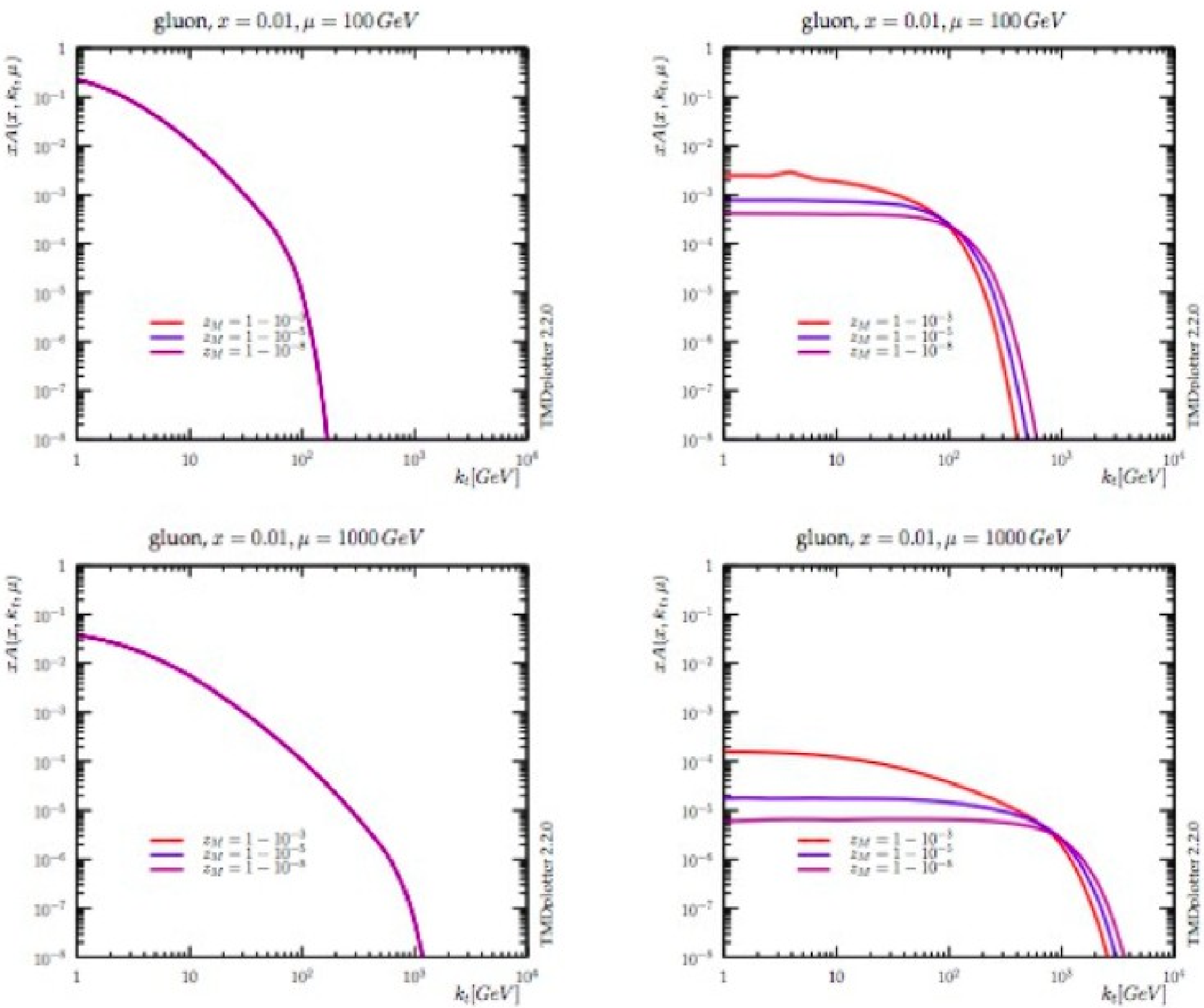

angular ordering

transverse momentum ordering

Well-defined TMDs require appropriate ordering condition

- Compare forward TMD evolution with backward evolution In parton shower with

  • Scale in alpha_s = qt

  • Resolution parameter zM = 1 – q0 / q'

[S Plaetzer et al, in progress]

PLB 772 (2017) 446

III. APPLICATIONS

PB method in xFitter

TMD distributions from fits to precision inclusive-DIS data from HERA using the open source QCD platform

xFitter [*S. Alekhin et al., E. Phys. J. C 75 (2014) 304*]

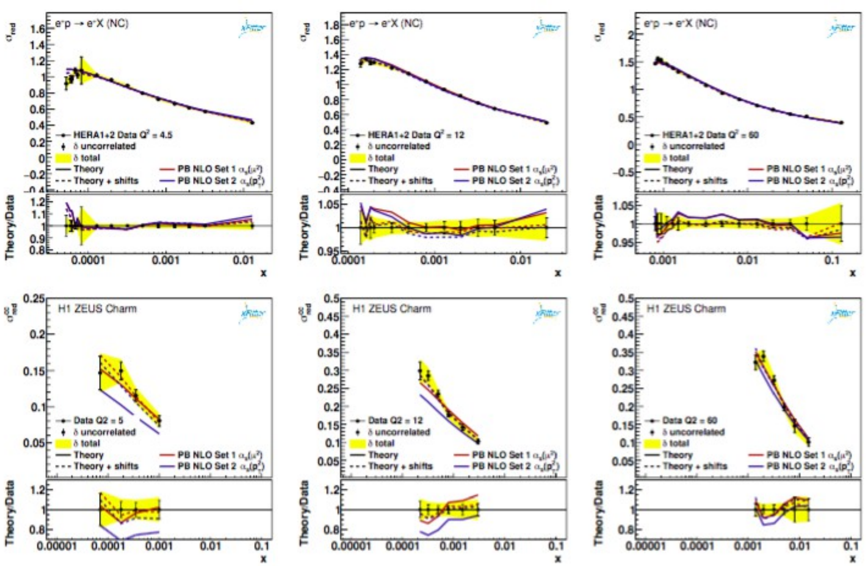

Figure 5: Measurement of the reduced cross section obtained at HERA compared to predictions using Set 1 and Set 2. Upper row: inclusive DIS cross section [11], lower row: inclusive charm production [38]. The dashed lines include the systematic shifts in the theory prediction.

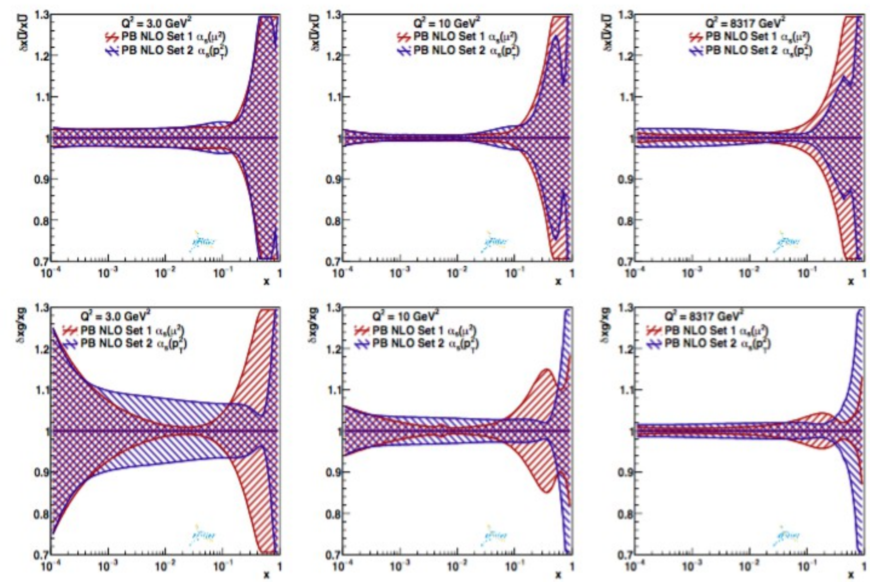

Figure 4: Total uncertainties (experimental and model uncertainties) for the two different sets at different values of the evolution scale μ^2.

A. Bermudez et al., Phys. Rev. D99 (2019) 074008

- NLO determination of TMDs including uncertainties

TMD distribution functions from precision DIS data fits

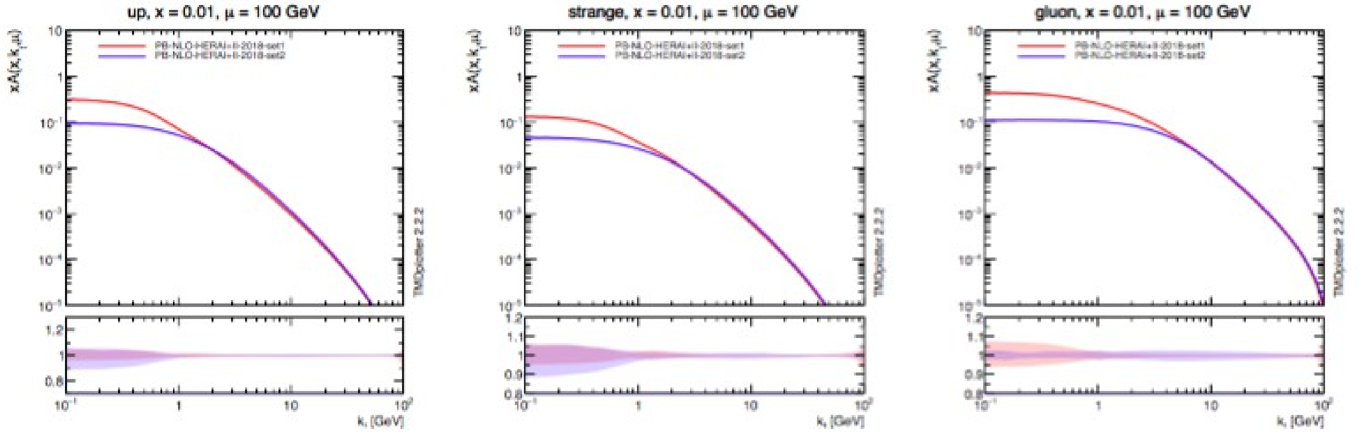

Figure 2: TMD parton distributions for up, strange and gluon (PB-NLO-2018-Set1 and PB-NLO-2018-Set 2) as a function of k_t at $\mu = 100$ GeVand $x = 0.01$.

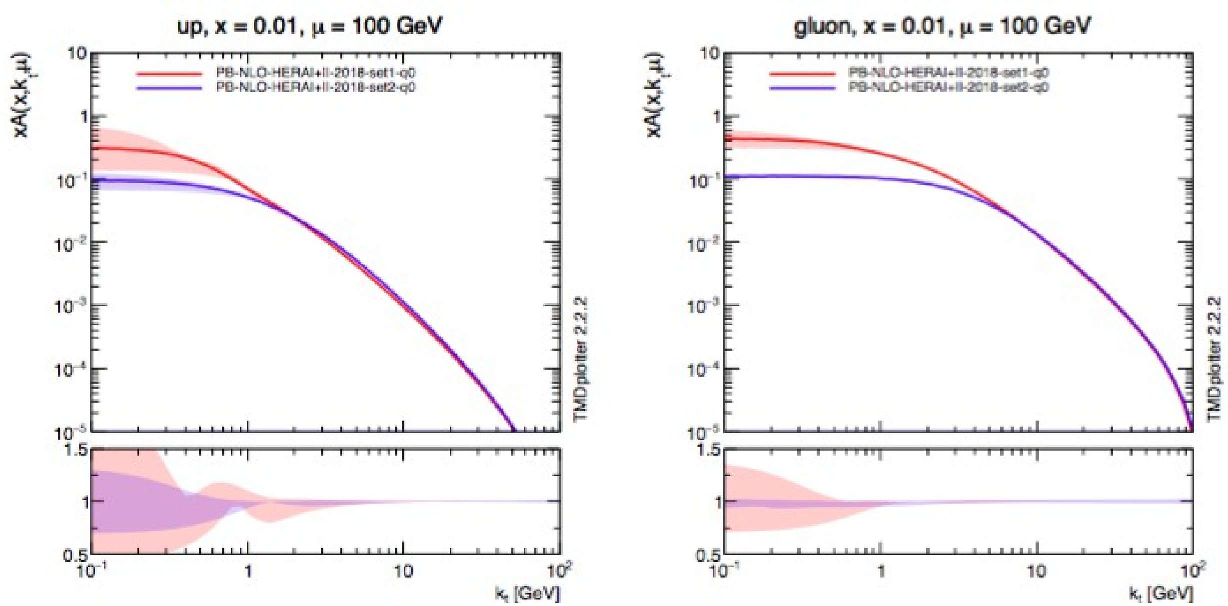

Figure 3: TMD parton distributions for up-quark and gluon (PB-NLO-2018-Set1 and PB-NLO-2018-Set 2) as a function of k_t at $\mu = 100$ GeVand $x = 0.01$ with a variation of the mean of the intrinsic k_t distribution.

3D Imaging and Monte Carlo

- **Parton Branching evolution**
  - start from hadron side and evolve from small to large scale μ^2

$$\Delta_s = \exp\left(- \int^{z_M} dz \int_{\mu_0^2}^{\mu^2} \frac{\alpha_s}{2\pi} \frac{d\mu'^2}{\mu'^2} P(z) \right)$$

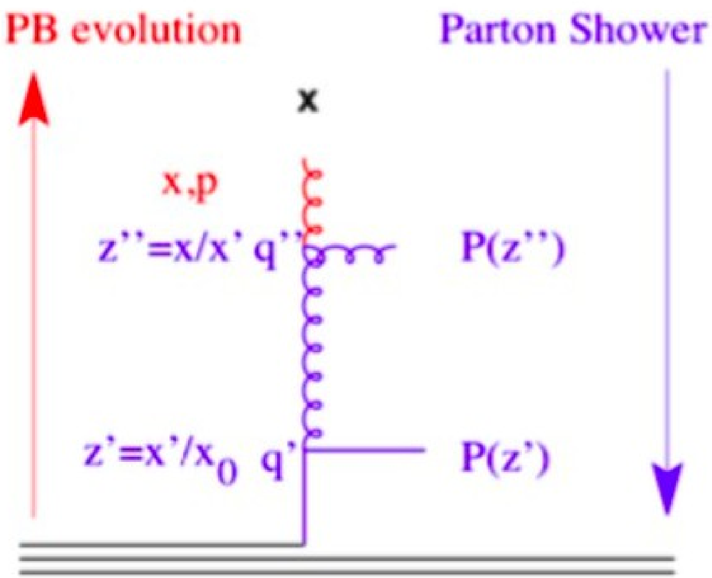

- **Parton Shower**
  - backward evolution from hard scale μ^2 to hadron scale μ^2_0 (for efficiency reasons)

$$\Delta_s = \exp\left(- \int^{z_M} dz \int_{\mu_0^2}^{\mu^2} \frac{\alpha_s}{2\pi} \frac{d\mu'^2}{\mu'^2} P(z) \frac{\frac{x}{z}\mathcal{A}\left(\frac{x}{z}, k'_\perp, \mu'\right)}{x\mathcal{A}(x, k_\perp, \mu')} \right)$$

➔ in backward evolution, parton density (TMD) imposed further constraint !

Z-boson DY production at the LHC:
TMDs fitted to inclusive DIS + NLO DY calculation

A Bermudez et al, arXiv:1906.00919

- Use MadGraph5_aMC-at-NLO
- Apply PB-TMD
- Set matching scale mu_m (kT < mu_m)

ATLAS 8 TeV data [E. Phys. J. C76 (2016) 291]

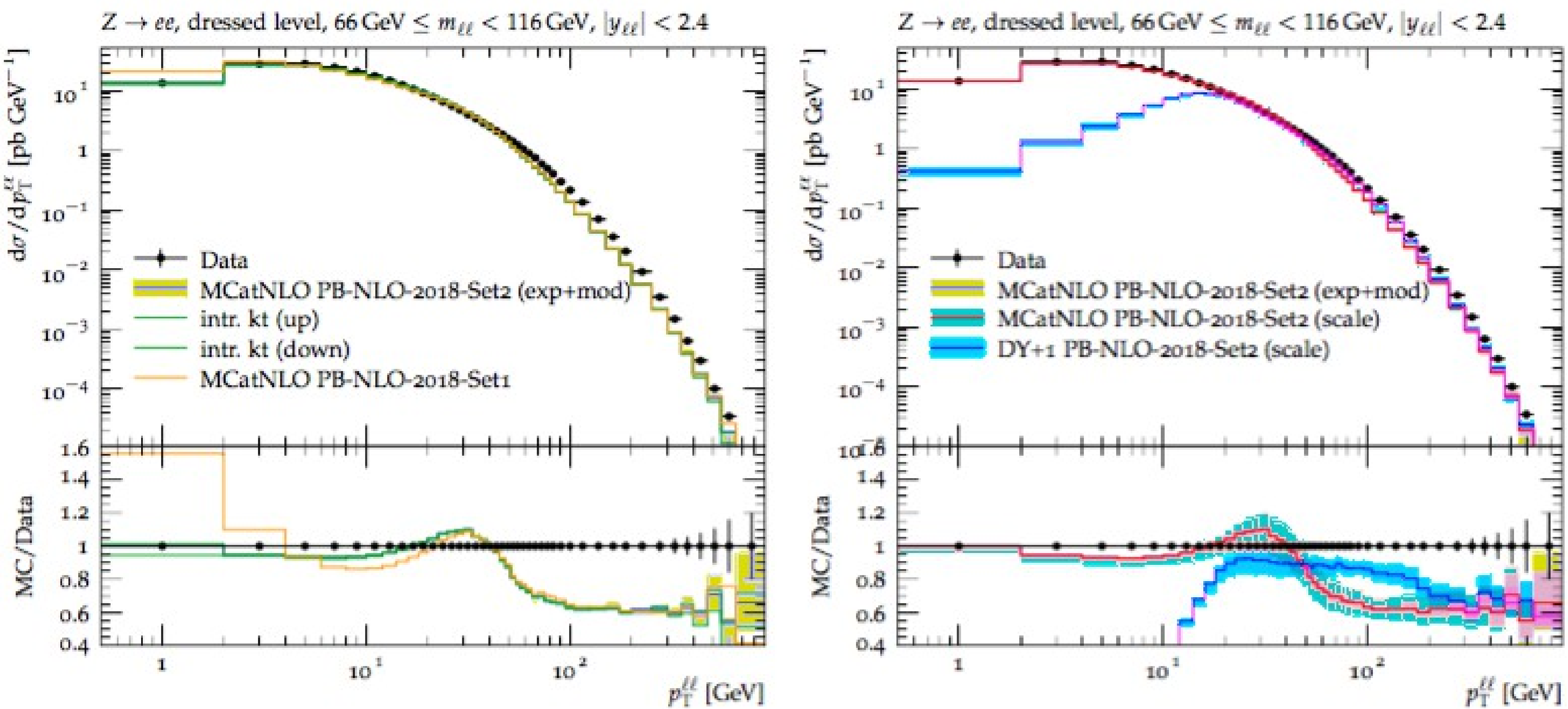

- Theoretical uncertainties dominated by scale dependences; TMD uncertainties moderate
- Low-pT spectrum sensitive to angular ordering (PB-TMD Set 2)
- Missing higher orders at high pT: see DY + 1 jet contribution

Z-boson DY production at the LHC:
TMDs fitted to inclusive DIS + NLO DY calculation

A Bermudez et al, arXiv:1906.00919

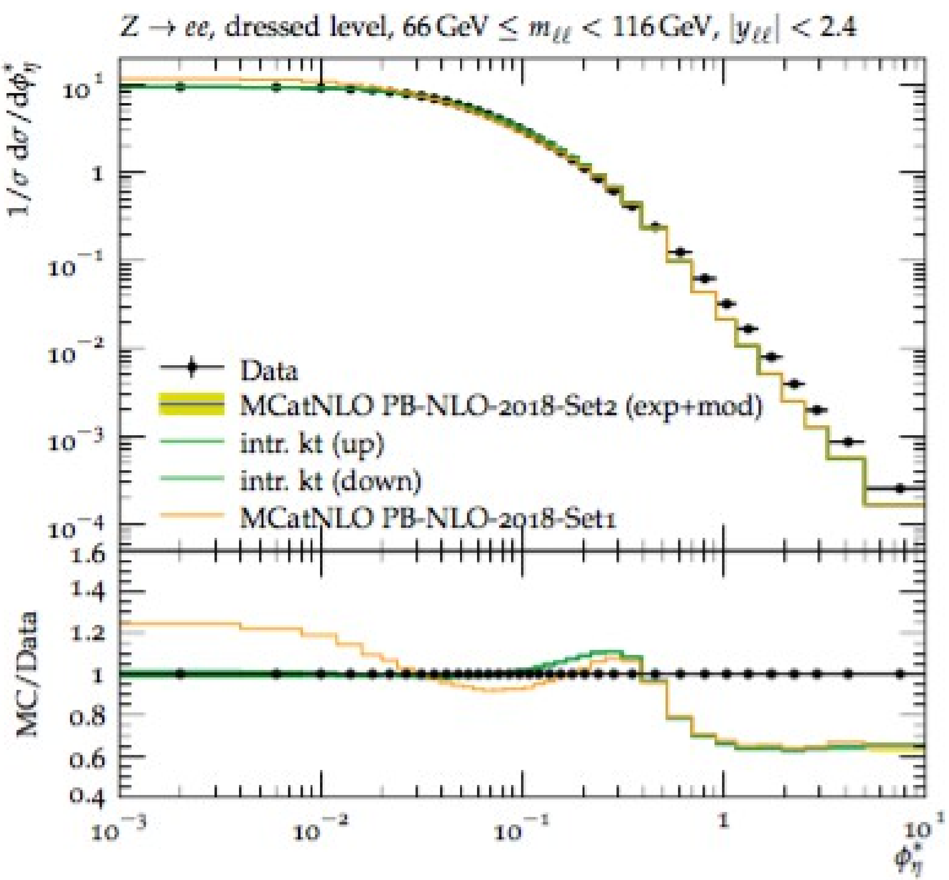

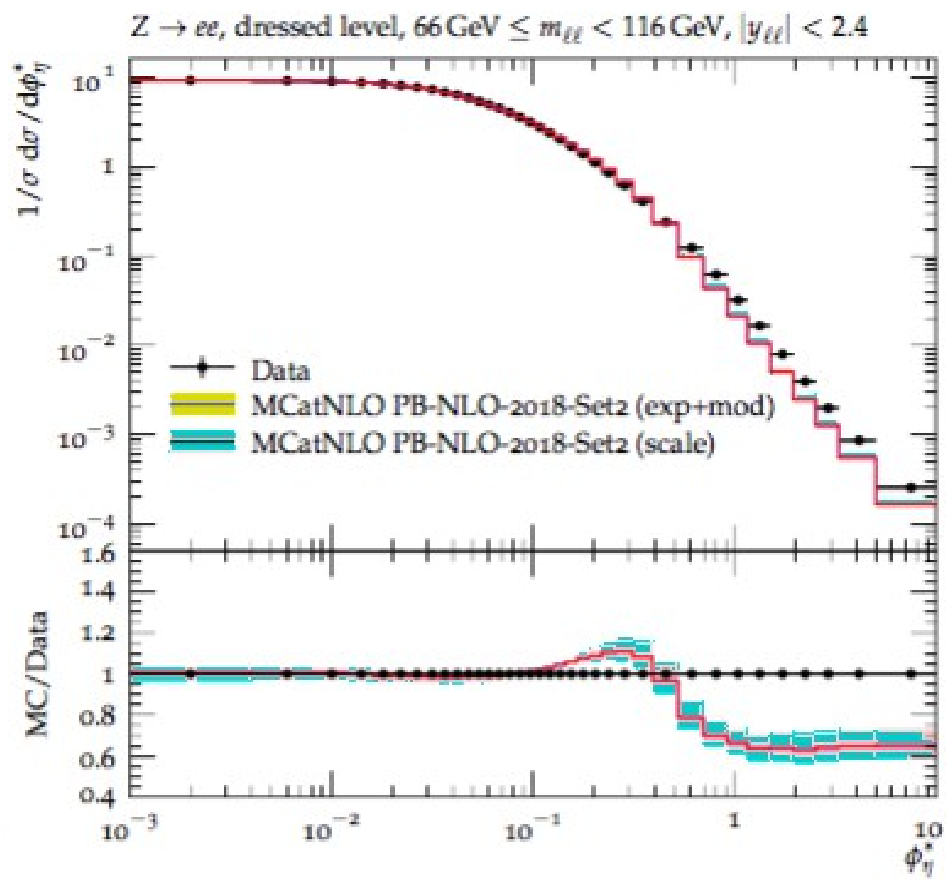

ATLAS 8 TeV data [E. Phys. J. C76 (2016) 291]

Predictions for 13 TeV

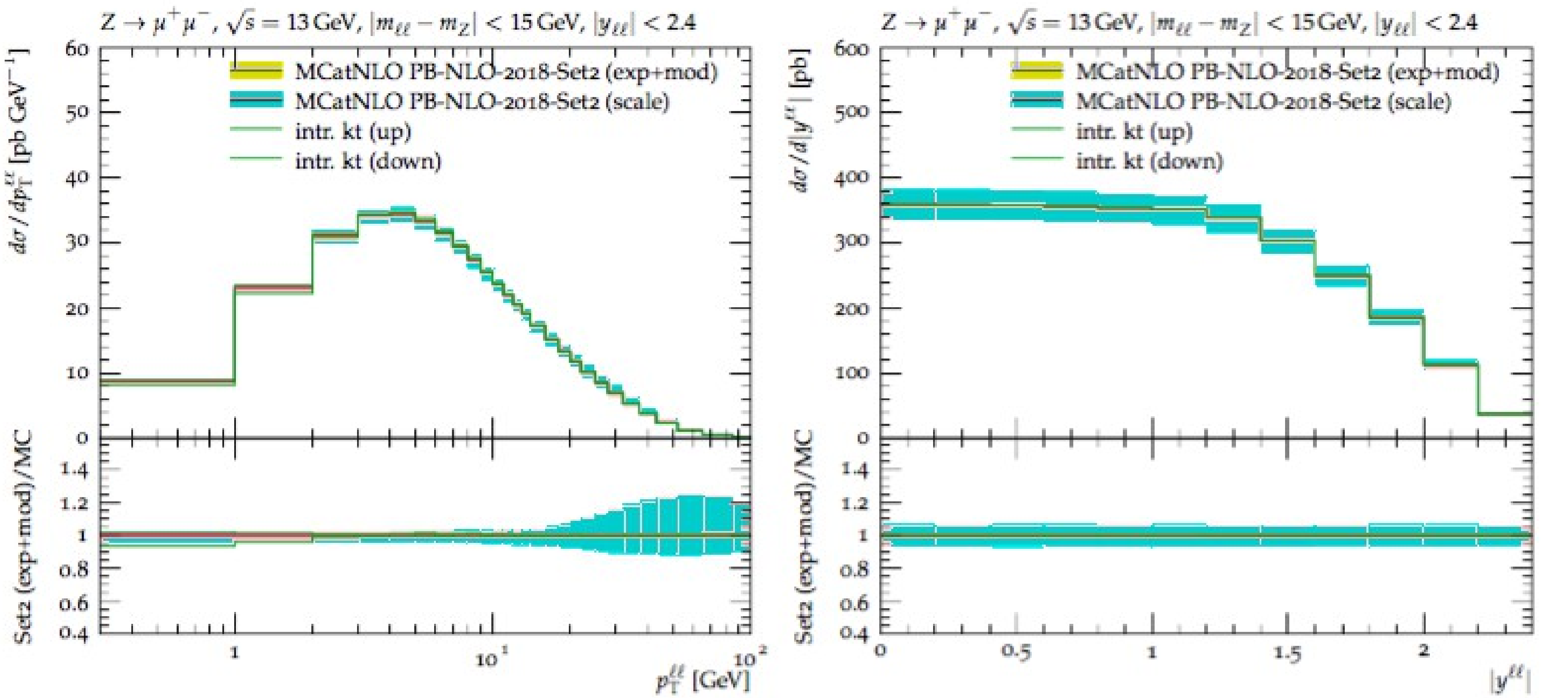

Figure 7: Transverse momentum p_T (left) and rapidity y spectra of Z-bosons at $\sqrt{s} = 13$ TeV from the prediction after including TMDs. The pdf (not visible) and the scale uncertainties are shown. In addition shown are predictions when the mean of the intrinsic gauss distribution is varied by a factor of 2 up and down.

Fine binning at low pT?

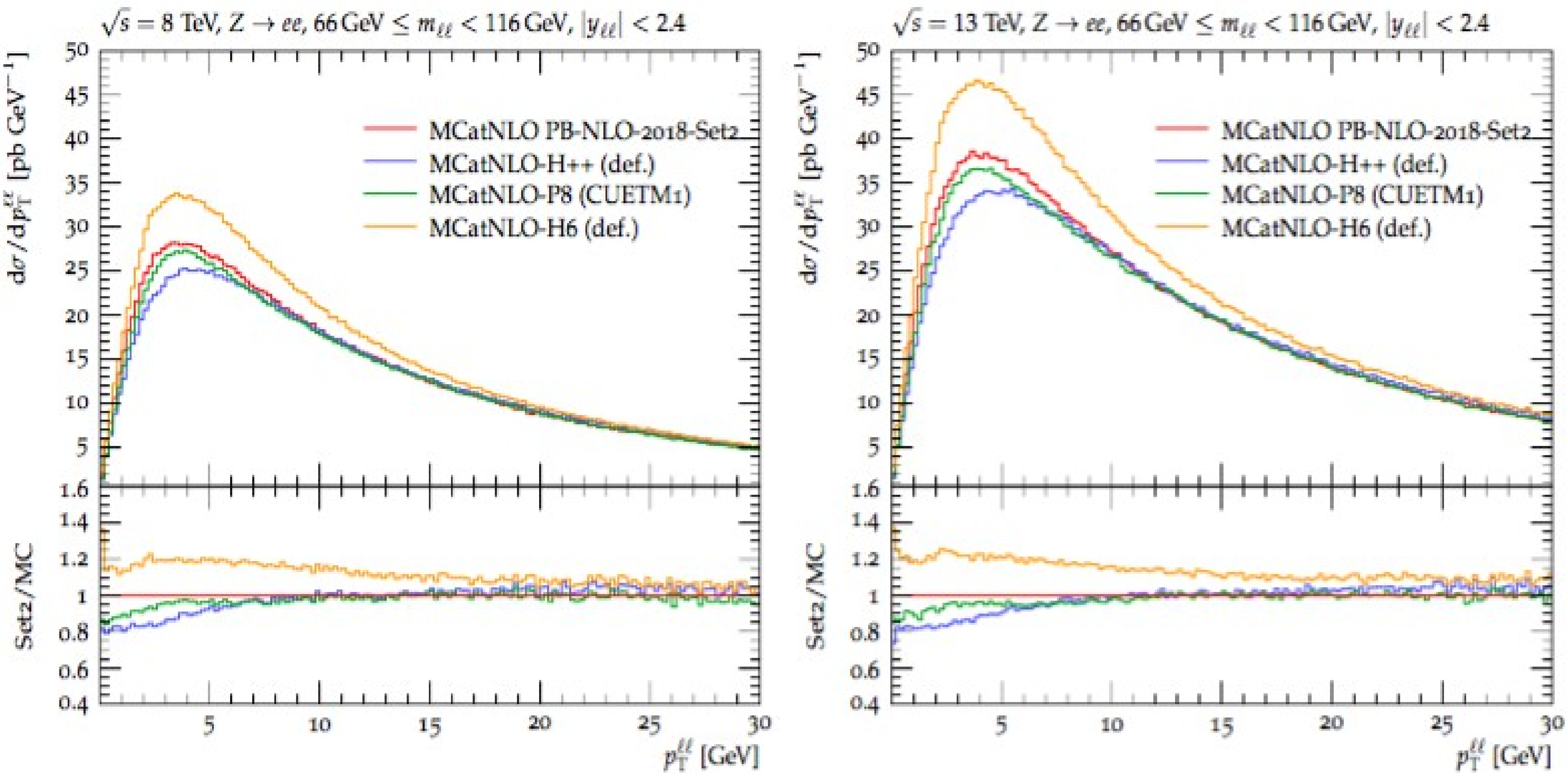

- dedicated measurements in the region of Z-boson pT < 5 -10 GeV?

Toward new approaches to matching/merging, locally in kT

Matching to hard process: off-shell ME with KaTie

van Hameren, A. CPC, 224, 371, 2018, arXiv 1611.00680

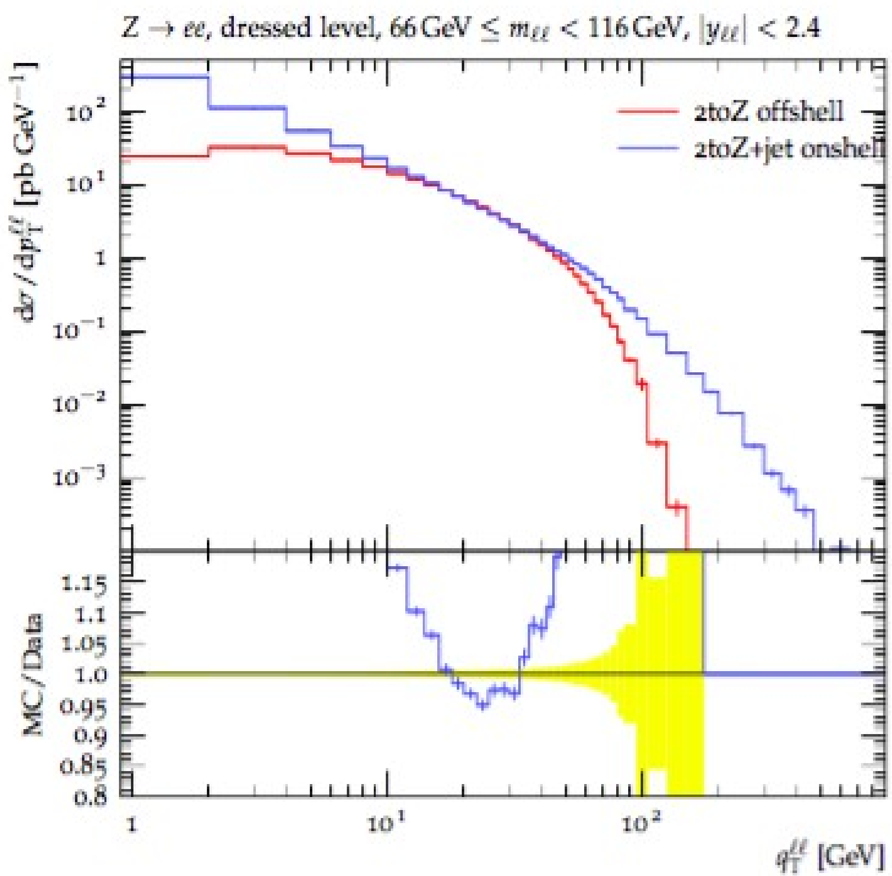

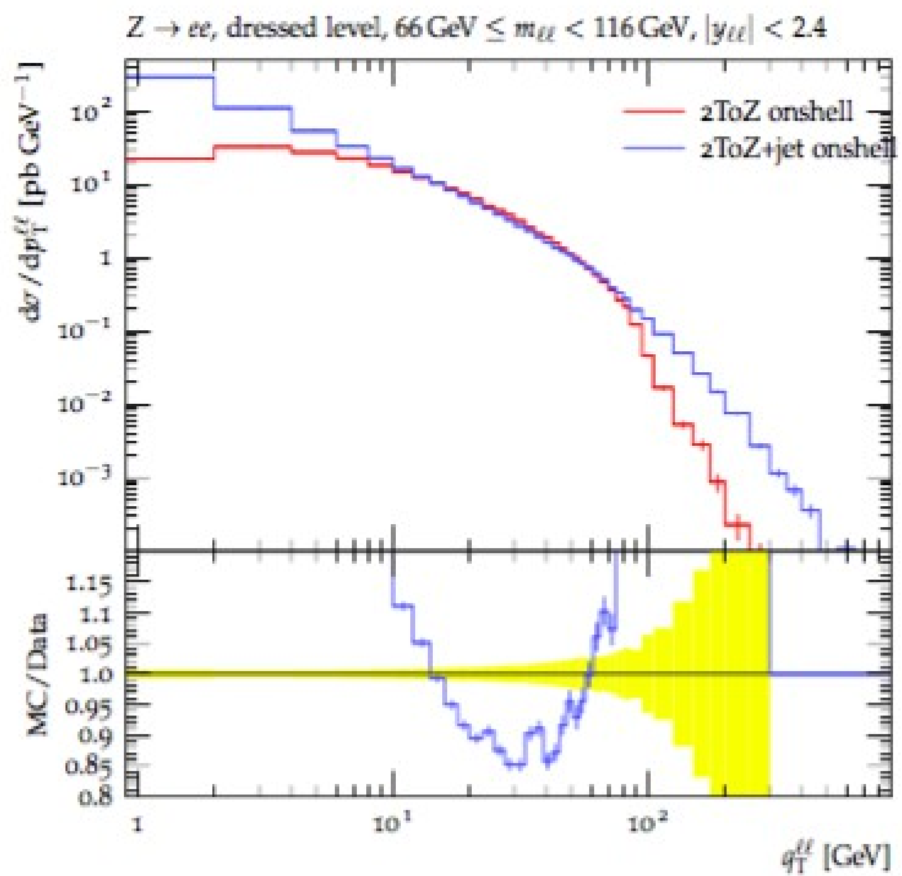

KaTie

[A. Van Hameren, talks at DESY MCEG Workshop, February 2019 and DIS2019 Workshop, April 2019]

Conclusions

- PB method to take into account simultaneously soft-gluon emission at z -> 1 and transverse momentum qT recoils in the parton branchings along the QCD cascade

- potentially relevant for calculations both in collinear factorization and in TMD factorization

  -> cf. parton shower calculations and analytic resummation

- terms in powers of ln (1 – zM) can be related to large-x resummation? -> relevant to near-threshold, rare processes to be investigated at high luminosity

- systematic studies of ordering effects and color coherence

  -> helpful to analyze long-time color correlations?